

УДК 539.1.07

EFFICIENCY PROFILE METHOD TO STUDY THE HIT EFFICIENCY OF DRIFT CHAMBERS

A. Abyzov^a, *A. Bel'kov*^a, *A. Lanyov*^a,
A. Spiridonov^b, *M. Walter*^b, *W. Hulsbergen*^c

^a Joint Institute for Nuclear Research, Dubna

^b DESY, Zeuthen, Germany

^c NIKHEF, Amsterdam

A method based on the usage of efficiency profile is proposed to estimate the hit efficiency of drift chambers with a large number of channels. The performance of the method under real conditions of the detector operation has been tested analysing the experimental data from the HERA-B drift chambers.

Для оценки эффективности срабатываний ячеек дрейфовых камер с большим количеством каналов предложен метод, основанный на использовании профильной функции эффективности. Применимость метода в реальных условиях работы детектора проверена на примере анализа экспериментальных данных с дрейфовых камер установки HERA-B.

INTRODUCTION

Two important characteristics of the performance of tracker detectors are their hit efficiency (the probability to register a signal in the cell after a passage of a charged particle) and track-finding efficiency (the probability to register a track of a charged particle). This paper is devoted to the study of the hit efficiency which is more relevant to the performance of the detector itself and the choice of its operating conditions. It also influences the track and trigger efficiencies.

The task of the hit efficiency determination by using results on track reconstruction with real experimental data becomes most important and complicated in case of modern tracker detectors which contain a large number of registering channels (more than hundred thousand channels). In this paper we describe a method of hit efficiency determination based on the usage of efficiency profiles. The standard reconstructed events can be used to produce these efficiency profiles. This is an advantage of the method because it does not need a special event reprocessing. To study the performance of this method under real conditions of operation of a large tracker detector, we have analysed the data taken in the year 2000 with the HERA-B [1] Outer Tracker (OTR) drift chambers.

The OTR uses honeycomb chambers with in total 1000 m² active area and 115 000 electronic channels providing the measurement of drift time. The inner diameter of the honeycomb cells is 5 mm for the part closest to the beam and 10 mm for the outermost region.

In this paper, systematic uncertainties of the efficiency profile method, related to the choice of track selection cuts, have been investigated. We have also studied possible efficiency bias due to the use of standard reconstruction, when the same set of cells is involved in the track finding and efficiency determination. Special Monte-Carlo studies have been performed to estimate the efficiency bias influenced by various reasons.

1. HIT EFFICIENCY PROFILE FUNCTION

Let us consider a track passing a cell with a small angle with respect to the Z axis at distance x to the anode wire so that an approximation $d \approx x$ is valid (see Fig. 1, where the cells of honeycomb drift chambers used in the HERA-B OTR are shown). Then the track length $l(x)$ inside the cell is given by

$$l(x) = \begin{cases} 2R \cos\left(\frac{\pi}{6}\right), & |x| < r; \\ 2(R - |x|) \operatorname{tg}\left(\frac{\pi}{3}\right), & r < |x| < R; \\ 0, & |x| > R; \end{cases}$$

where R and r are defined in Fig. 1. Assuming that the number of ionization clusters produced by a particle is described by Poisson statistics, the probability for a track to have n clusters within a cell is defined as

$$P(n) = \frac{(\alpha l)^n}{n!} e^{-\alpha l},$$

where α is an «effective» cluster density. The word «effective» means that we consider only the clusters that are registered. As a consequence, $P(0) = e^{-\alpha l}$ and the probability to create at least one cluster is given by

$$P(n > 0) = 1 - e^{-\alpha l}.$$

With these assumptions the hit efficiency profile function can be written as

$$\varepsilon(x) = 1 - e^{-\alpha l(x)}.$$

It is more convenient to parameterize this function in the following form:

$$\varepsilon(x) = \begin{cases} \varepsilon_{\max}, & |x| < r; \\ 1 - e^{-\lambda(R-|x|)}, & r < |x| < R; \\ 0, & |x| > R; \end{cases}$$

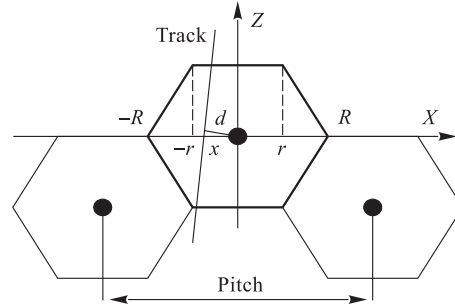


Fig. 1. Honeycomb drift cells structured as a single layer which is sensitive over the whole x - y plane. The cell under study is drawn by bold lines. $R = \text{pitch}/3$, $r = R/2$

with the condition $\varepsilon_{\max} = 1 - e^{-\lambda(R-r)}$, where $\lambda = 2\alpha \operatorname{tg}(\pi/3)$. After some algebraic manipulation, one obtains the ideal hit efficiency profile

$$\varepsilon_{\text{ideal}}(x) = \begin{cases} \varepsilon_{\max}, & |x| < r; \\ 1 - \exp\left(-\gamma \frac{R-|x|}{R-r}\right), & r < |x| < R; \\ 0, & |x| > R; \end{cases} \quad (1)$$

with $\gamma = -\ln(1 - \varepsilon_{\max})$ (see Fig. 2, where a typical shape of the ideal profile function is shown).

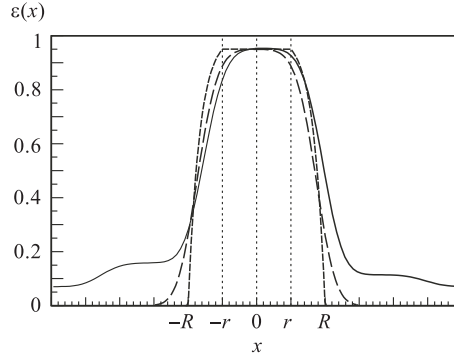


Fig. 2. Example of efficiency profile function in various approximations: the dotted line shows the ideal efficiency profile describing the cluster statistics by Eq. (1); the dashed line corresponds to the efficiency profile smeared according to Eq. (2); the solid line shows the efficiency profile function (8) taking into account background, cross talk, and misalignment

In real measurements, a hit efficiency profile is smeared due to the errors in the track parameter determination. In case of Gaussian smearing, the corresponding efficiency profile is

$$\varepsilon_{\text{meas}}(x) = \int_{-\infty}^{+\infty} \varepsilon_{\text{ideal}}(y) \frac{1}{\sqrt{2\pi}\sigma} \exp\left(-\frac{(x-y)^2}{2\sigma^2}\right) dy. \quad (2)$$

In Fig. 2, the smeared efficiency profile is compared with the ideal one. Dividing in Eq. (2) the limits of integration according to different cases in Eq. (1), one gets

$$\varepsilon_{\text{meas}}(x) = \int_{-R}^{-r} \varepsilon_{\text{ideal}}(y) G(y; x, \sigma) dy + \int_{-r}^r \varepsilon_{\text{ideal}}(y) G(y; x, \sigma) dy + \int_r^R \varepsilon_{\text{ideal}}(y) G(y; x, \sigma) dy, \quad (3)$$

where $G(y; x, \sigma) \equiv \frac{1}{\sqrt{2\pi}\sigma} \exp\left(-\frac{(x-y)^2}{2\sigma^2}\right)$.

Now let us calculate each term in Eq. (3) separately. The function $F(y', x, \sigma) = \int_{-\infty}^{y'} G(y; x, \sigma) dy$ is the standard error function computed rather fast by rational Chebyshev approximation. So, we have

$$\int_{-r}^r \varepsilon_{\text{ideal}}(y) G(y; x, \sigma) dy = \varepsilon_{\text{max}} [F(r, x, \sigma) - F(-r, x, \sigma)], \quad (4)$$

$$\begin{aligned} \int_r^R \varepsilon_{\text{ideal}}(y) G(y; x, \sigma) dy &= \int_r^R \left(1 - \exp\left(-\gamma \frac{R-y}{R-r}\right) \right) G(y; x, \sigma) dy = \\ &= \int_r^R G(y; x, \sigma) dy - \exp\left(-\gamma \frac{R-x}{R-r}\right) \int_r^R \exp\left(-\gamma \frac{x-y}{R-r}\right) G(y; x, \sigma) dy = \\ &= F(R, x, \sigma) - F(r, x, \sigma) - \exp\left(-\gamma \frac{R-x}{R-r}\right) \int_{r-x}^{R-x} \tilde{G}\left(y; \frac{\gamma}{R-r}, 0, \sigma\right) dy, \end{aligned} \quad (5)$$

$$\begin{aligned} \int_{-R}^{-r} \varepsilon_{\text{ideal}}(y) G(y; x, \sigma) dy &= \int_{-R}^{-r} \left(1 - \exp\left(-\gamma \frac{R+y}{R-r}\right) \right) G(y; x, \sigma) dy = \\ &= \int_r^R \left(1 - \exp\left(-\gamma \frac{R-y}{R-r}\right) \right) G(y; -x, \sigma) dy = F(R, -x, \sigma) - F(r, -x, \sigma) - \\ &\quad - \exp\left(-\gamma \frac{R+x}{R-r}\right) \int_{r+x}^{R+x} \tilde{G}\left(y; \frac{\gamma}{R-r}, 0, \sigma\right) dy, \end{aligned} \quad (6)$$

where $\tilde{G}(y; c, x, \sigma) \equiv e^{cy} \frac{1}{\sqrt{2\pi}\sigma} \exp\left(-\frac{(x-y)^2}{2\sigma^2}\right)$ and

$$\begin{aligned} \int_{-\infty}^{y'} \tilde{G}(y; c, 0, \sigma) dy &= \int_{-\infty}^{y'} e^{cy} \frac{1}{\sqrt{2\pi}\sigma} \exp\left(-\frac{y^2}{2\sigma^2}\right) dy = \\ &= \exp\left(\frac{c^2\sigma^2}{2}\right) \int_{-\infty}^{y'-c\sigma^2} G(y; 0, \sigma) dy = \exp\left(\frac{c^2\sigma^2}{2}\right) F(y', 0, \sigma). \end{aligned} \quad (7)$$

From Eqs. (4)–(7) we see that the measured efficiency profile function (2) can be expressed in terms of the error function $F(y', x, \sigma)$.

The response from the cell can be caused either by the track passing the cell, or by the background event, or by the cross talk from the left and right neighbouring cells. We consider all these processes to be independent. Then, the probability to get some response from the cell, $P_{\text{hit}}(x)$, while the track passes the cell at distance x from the wire, can be estimated as

$$P_{\text{hit}}(x) = 1 - [1 - \varepsilon_{\text{meas}}(x + \Delta x)](1 - P_{\text{bg}})[1 - P_{\text{ctl}}(x)][1 - P_{\text{ctr}}(x)], \quad (8)$$

where Δx is a shift in x coordinate due to the drift chamber misalignment; P_{bg} is probability of the background; P_{ctl} (P_{ctr}) is probability of the cross talk from the left (right) cell expressed as profile function (2) multiplied by value C_{ctl} (C_{ctr}) and shifted by $\frac{3}{2}R$ to the left (right) on X axis, i. e.,

$$P_{\text{ctl}}(x) = C_{\text{ctl}}\varepsilon_{\text{meas}}\left(x + \frac{3}{2}R + \Delta x\right), \quad P_{\text{ctr}}(x) = C_{\text{ctr}}\varepsilon_{\text{meas}}\left(x - \frac{3}{2}R + \Delta x\right).$$

Figure 2 shows the typical shape of the efficiency profile given by Eq. (8), which takes into account the background, cross talk, and misalignment.

2. METHOD TO STUDY HIT EFFICIENCY

Let us denote the total number of track segments passing the cell by N^{exp} , and the number of hits in the cell by N^{real} . Each time a segment passes through the cell, the number N^{exp} is incremented by one and, if there is a hit in the cell, the number N^{real} is also incremented by one. The hit efficiency of a cell is determined as the ratio

$$\varepsilon_{\text{hit}} = N^{\text{real}}/N^{\text{exp}}. \quad (9)$$

Each selected track segment is fitted by a straight line. For each cell two histograms are filled, $N^{\text{real}}(d)$ and $N^{\text{exp}}(d)$, corresponding to the track distance distributions of real and expected numbers of hits, respectively, where d is a distance from the segment to the wire. Then, the efficiency profile was calculated as the ratio

$$P_{\text{hit}}(d) = N^{\text{real}}(d)/N^{\text{exp}}(d). \quad (10)$$

A typical example of the efficiency profile histogram with fitting function is shown in Fig. 3.

To fit the histogram in Fig. 3, we have used Eq. (8) as a fitting function. The following parameters can be determined from the experimental histogram for the efficiency profile (10):

- ε_{max} — maximal value of the ideal hit efficiency profile;
- σ — RMS of smearing due to the error in track parameters;
- P_{bg} — value of background;
- C_{ctl} — probability to register a cross-talk signal from the left neighbouring cell;
- C_{ctr} — probability to register a cross-talk signal from the right neighbouring cell;
- Δx — shift in x coordinate due to misalignment.

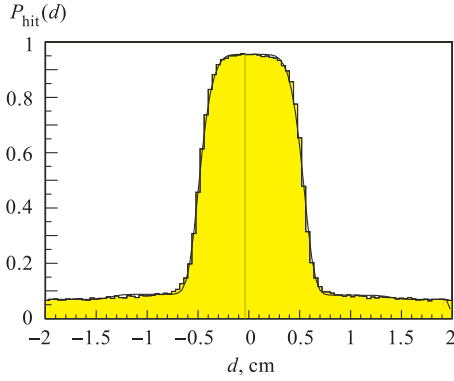


Fig. 3. Example of efficiency profile histogram and fitting function for 10-mm drift cells of the HERA-B tracker

According to Eq. (8), the value of ε_{\max} corresponds to the real cell efficiency rather than to a sum of the cell efficiency and background P_{bg} . Then, the cell efficiency is determined as the value of parameter ε_{\max} .

The smearing due to errors in track parameters and the shift due to misalignment are not relevant directly to the hit efficiency. Because of the limited statistics and small cross-talks, the values $C_{\text{ctl}(r)}$ are consistent very often with zero for separate cells. Therefore, only two parameters of the fitting function will be presented and discussed: ε_{\max} and P_{bg} .

3. DATA ANALYSIS

The method of hit efficiency determination described in sections 1 and 2 has been tested when studying the performance of the OTR chambers of the HERA-B set-up in a run during the HERA-B commissioning period in the year 2000 at an interaction rate of 5 MHz. During this commissioning phase the main tracker detectors were still not perfect; for example, about 12% of the OTR channels were turned off or very noisy. Certainly, these «bad» cells were excluded from the analysis and did not influence directly the values of hit efficiency, but the tracking efficiency and possible failures of pattern recognition were affected [2]. Also the high voltage was lower than the optimal and, therefore, hit efficiencies were smaller than designed ones [3].

The OTR of HERA-B consists of honeycomb drift cells and is divided into three groups of superlayers: pattern chambers (PC), trigger chambers (TC), and magnet chambers (MC). The complicated modular geometry of the OTR is described in [4]. The PC and TC chambers (located downstream of the magnet) are grouped in four and two superlayers, respectively: PC1–PC4 and TC1–TC2. Each of them consists of two separate gas boxes in the left ($-x$ half of superlayer) and right ($+x$ half) sides of the proton beam pipe. The coordinate system indicated in Fig. 1 is used: the Z axis goes along the proton beam; the X axis is directed horizontally to the right when looking towards increasing z coordinate, and the Y axis completes the orthogonal system. The position of the target is $z \approx 0$ and the centre of the magnet is located at approximately 450 cm.

Each PC superlayer has six stereolayers oriented by different stereoangles ($\alpha = 0^\circ, -4.6^\circ, +4.6^\circ$). The stereolayers consist of modules with a single or double layer of hexagonal cells. The straight line passing through this honeycomb module traverses at least one cell in a single layer (see Fig. 1). The number of the single layers is 30 in the PC chambers, and 12 in the TC chambers.

For the reconstruction of track segments in the PC and TC regions, the program Ranger [5], the ARTE environment [6] and standard hit preparation have been used. Distributions of parameters used for track selection are shown in Fig. 4. In the present paper, to demonstrate the method performance, we will present only the results for $-x$ halves of PC superlayers obtained from the analysis of run 14577 (minimum-bias events). For more technical details on hit efficiency studies performed recently for the OTR superlayers by using the efficiency profile method, see Ref. [3].

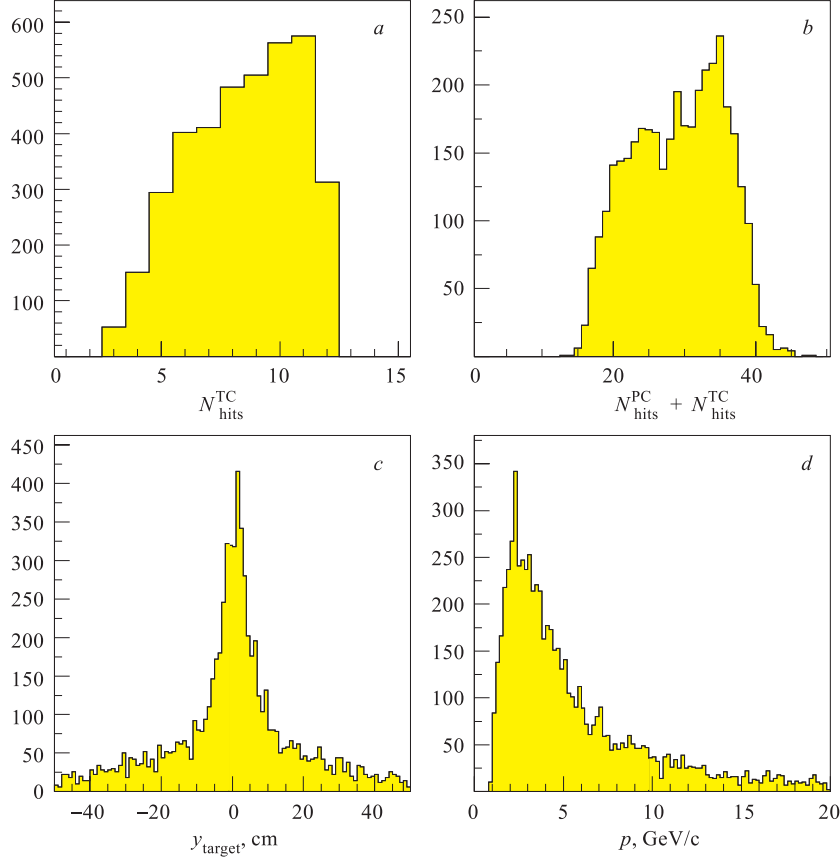


Fig. 4. Distribution of parameters used for track selection: *a)* $N_{\text{hits}}^{\text{TC}}$; *b)* $N_{\text{hits}}^{\text{PC}} + N_{\text{hits}}^{\text{TC}}$; *c)* y_{target} , and *d)* p . The meaning of the parameters is described in the text

In the analysis we have used only events where the total number of hits per event is $900 < N_{\text{hits}} < 8000$ in the OTR chambers. Only segments with momenta $p > 3 \text{ GeV}/c$ have been selected. To study how much the evaluated hit efficiency depends on the selection criteria, we have used two sets of additional cuts for track selection:

- Soft cuts:
 - Only segments with $|y_{\text{target}}| < 25 \text{ cm}$, where y_{target} is y coordinate of the segment prolonged to the target region $z = 0$, were selected.
 - Only those PC segments that have a matched segment in TC chambers were used.
 - The number of hits in TC per segment is required to be $N_{\text{hits}}^{\text{TC}} > 6$.
 - The number of hits in PC + TC per segment is required to be $N_{\text{hits}}^{\text{PC}} + N_{\text{hits}}^{\text{TC}} > 20$.

- Strong cuts:
 - Only PC segments that have matched segments both in TC and in vertex detector (located upstream of the magnet) were used.
 - The number of hits in TC is required to be $N_{\text{hits}}^{\text{TC}} > 9$.
 - The number of hits in PC is required to be $N_{\text{hits}}^{\text{PC}} > 24$.

It should be mentioned that the cell under study was not included in counting hits, since this can bias the results.

The superlayer efficiency has been determined as an average of the cell efficiency distribution for cells in the superlayer. To estimate the superlayer efficiency, the following selection criteria on cells in the superlayer have been applied (see Fig. 5):

- Only «good» cells, according to Data Quality¹, have been taken into account.
- Only cells with the hit efficiency higher than 0.75 have been included in the distribution.
- Only cells with «good» χ^2 , e. g., $0.4 < \chi^2 < 1.5$, have been taken into account.

The second criterion needs some explanation. Applying this criterion, we want to reject bad cells that were not identified properly by Data Quality package. The contribution of these cells is seen in Fig. 5, *a* for ε close to zero. The value of the cut has been chosen after studying the dependence of the average hit efficiency of the superlayer as a function of the cut on the minimal cell efficiency shown in Fig. 6, *a*. The evaluated efficiencies look quite stable for a cut parameter smaller than 0.75.

The average hit efficiencies ε_{hit} and background probabilities P_{bg} for PC superlayers, estimated from the data analysis by using soft and strong cuts of track selection, are presented in Table 1. Figure 6, *b* shows the distribution of hit efficiencies for 5-mm cells of different PC superlayers, obtained with soft cuts for track selection. From Table 1 one can notice that the hit efficiency for 10-mm cells is higher than for 5-mm cells. The value of the background probability varies from 4 to 8 %. The average occupancy in the OTR (the ratio of the average number of hits to the number of cells) is about 4 % for this run. The background becomes higher for larger z coordinates because of secondary interactions in the detector material.

To see the hit efficiency in different parts of the detector, we have studied variation of the efficiencies for different GEDE², which is shown in Fig. 7 for both the soft and strong cuts of track selection. It is seen that the hit efficiency values determined with the strong cuts are more stable in different parts of the detector than with the soft cuts. It was also observed that the efficiencies became worse for the modules that are closer to the beam pipe. This fact can be partially explained by the failures of track finding in the region of the higher track density. The background level, χ^2 and σ for efficiency profiles are worse as well for those modules.

¹Data Quality is the software package that determines the bad cells.

²A single unit of the sensitive detector volume is called GEDE (GEometry DETector). In OTR, a physical module is divided into several GEDE volumes.

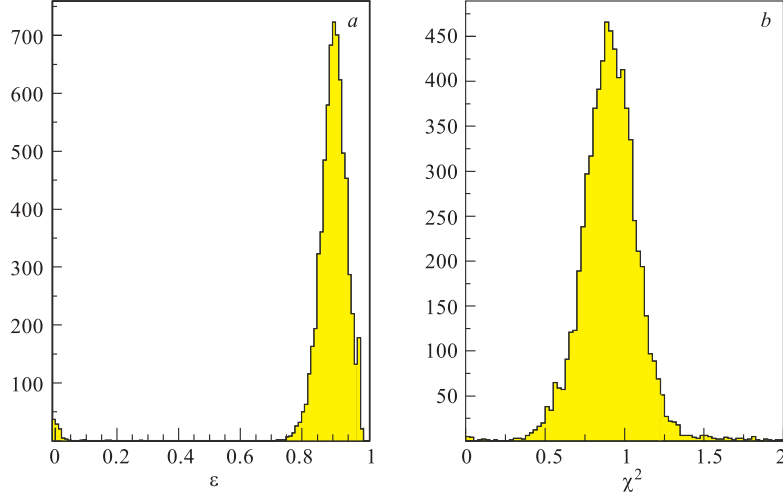


Fig. 5. Distributions of hit efficiency (a) and χ^2 (b) for 5-mm cells in PC1 superlayer (only for good cells, according to Data Quality)

Table 1. Hit efficiencies ε_{hit} and background probabilities P_{bg} (in %) for PC superlayers obtained from the data analysis with the soft and strong cuts for track selection

Superlayer	Quantity	Soft cut		Strong cut	
		5 mm	10 mm	5 mm	10 mm
PC1	ε_{hit}	90.2 (4.1)	92.2 (3.7)	94.5 (3.7)	95.9 (2.9)
	P_{bg}	4.5 (2.3)	5.1 (1.5)	3.9 (2.0)	4.6 (2.2)
PC2	ε_{hit}	90.7 (3.9)	94.5 (2.5)	96.7 (2.5)	97.9 (1.7)
	P_{bg}	5.6 (2.7)	6.0 (1.6)	4.3 (1.9)	5.5 (2.4)
PC3	ε_{hit}	90.8 (4.1)	95.6 (2.1)	96.3 (2.8)	98.2 (1.6)
	P_{bg}	6.4 (3.0)	6.7 (1.7)	4.7 (2.0)	5.7 (2.4)
PC4	ε_{hit}	92.7 (3.6)	94.0 (3.0)	95.4 (3.6)	95.1 (3.7)
	P_{bg}	7.4 (3.7)	7.4 (2.1)	5.5 (2.5)	6.4 (2.7)

Note. Numbers in brackets denote the RMS of the distributions of corresponding parameters for separate cells in the superlayer. Statistical errors are negligible due to a big number of events.

4. ESTIMATION OF EFFICIENCY BIAS

The values for the hit efficiency estimated above can be biased for the following reasons:

- The same hits as used at first to define a track are taken then to estimate the hit efficiency.

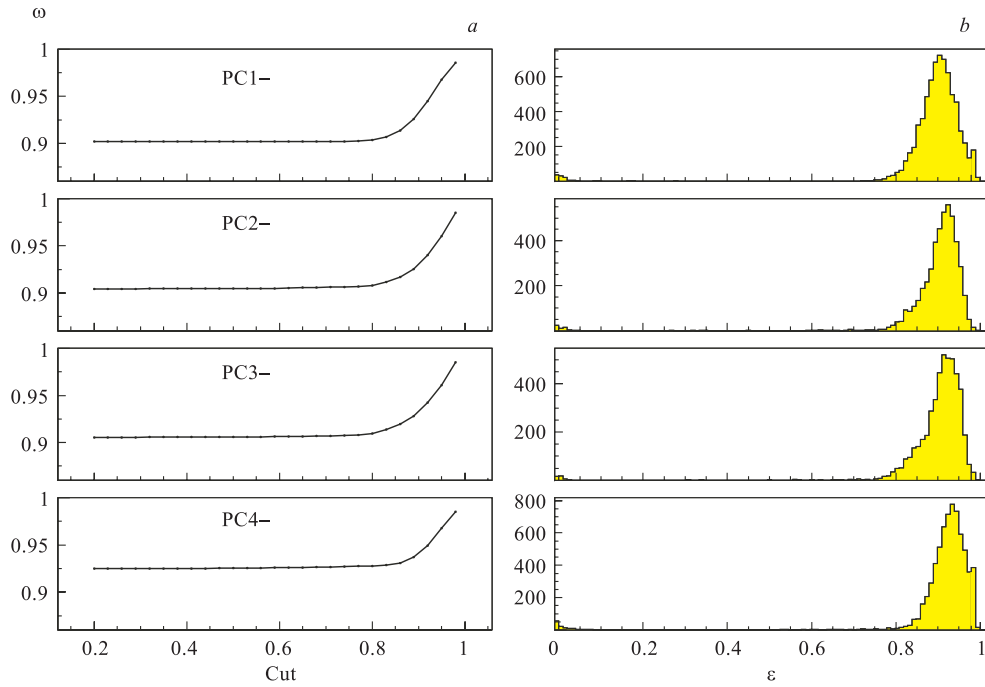


Fig. 6. Results of hit efficiency analysis for different superlayers, obtained for the data: *a*) the average hit efficiency of a superlayer as a function of the value of the cutoff on the cell efficiency; *b*) distribution of efficiency of 5-mm cells (only good cells, according to Data Quality, were included)

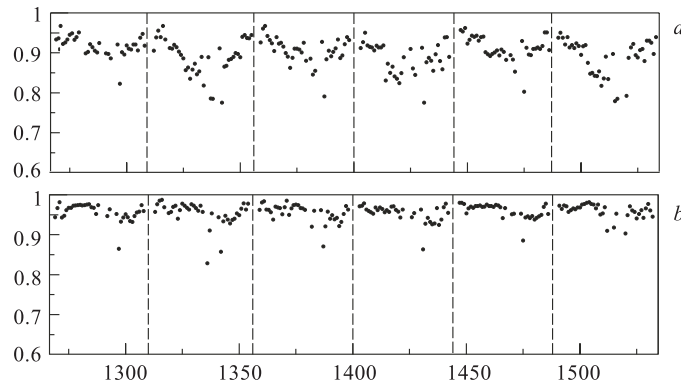


Fig. 7. Hit efficiency as a function of the GEDE number (of the OTR module) in the PC2 superlayer for soft (*a*) and strong (*b*) cuts of track selection. Vertical lines separate different stereolayers. The GEDE volumes are enumerated in such a way that the middle of the stereolayer corresponds to the region close to the beam

- There is a fraction of ghosts in the reconstructed track sample.

The bias in the hit efficiency determination, caused by the first reason, can be estimated by excluding some set of cells from tracking and evaluating the unbiased hit efficiency. For this purpose, the first stereolayer of PC2 has been excluded from tracking. The track selection criteria have also been slightly changed; i. e., the number of hits in PC + TC was required to be $N_{\text{hits}}^{\text{PC}} + N_{\text{hits}}^{\text{TC}} > 19$. All the other conditions were not changed. Table 2 shows the values of bias of hit efficiency $\Delta\varepsilon = \varepsilon_{\text{new}} - \varepsilon_{\text{old}}$, where ε_{old} and ε_{new} are hit efficiencies before and after exclusion of the first stereolayer, respectively. One can see that there is a bias for the excluded stereolayer; however, its value is below 1 %.

The bias study for hit efficiency determination has also been performed by using Monte-Carlo simulation of the detector under the following conditions:

- Mean number of inelastic Poisson-distributed interactions on the target wire per event was equal to 2.7.
- OTR chamber resolution is 500 μm .
- Cells corresponding to bad channels in the data were excluded (about 12 %).
- OTR hit efficiency is 95 %.

The results for efficiencies of different PC superlayers show in Table 3 that efficiency determination is biased especially for the chambers with 5-mm cells. The values of the background P_{bg} determined by means of Monte-Carlo simulation are in agreement within 1–2 % with those obtained from the real data analysis. At the same time one can see that the background increases with increasing the superlayer number (i. e., with increasing z coordinate) faster for the real data (see Table 1) than for Monte-Carlo simulation. The efficiency values obtained in Monte-Carlo simulation with strong cuts are much closer to the input value 95 %. Also the values of RMS of efficiency distribution in Table 3 indicate that the systematic error of the efficiency determination is of the order of 2–3 %. This systematic error partially depends on the failure in track finding due to the high level of bad cells. We hope that the situation will be improved in future, since a large fraction of the nonworking and noisy channels have been repaired.

Table 2. Estimate of bias in hit efficiency $\Delta\varepsilon$ (in %) of various PC2 stereolayers for the data

Stereo-layer	PC2–		Stereo-layer	PC2–	
	5 mm	10 mm		5 mm	10 mm
1*	-0.8 ± 0.25	-0.4 ± 0.55	4	-0.1 ± 0.3	-0.1 ± 0.7
2	$+0.3 \pm 0.3$	-0.1 ± 0.4	5	-0.05 ± 0.2	-0.05 ± 0.3
3	$+0.1 \pm 0.15$	-0.05 ± 0.6	6	-0.25 ± 0.3	-0.35 ± 0.4

* The excluded stereolayer.

Table 3. Hit efficiencies ε_{hit} and background probabilities P_{bg} (in %) for PC superlayers estimated for Monte-Carlo events with the soft and strong cuts for track selection

Superlayer	Quantity	Soft cut		Strong cut	
		5 mm	10 mm	5 mm	10 mm
PC1	ε_{hit}	91.5 (3.4)	93.2 (2.9)	93.8 (3.3)	94.6 (2.9)
	P_{bg}	3.8 (1.7)	5.0 (2.2)	3.5 (1.4)	4.7 (2.5)
PC2	ε_{hit}	91.6 (3.1)	93.5 (2.2)	95.0 (2.5)	95.3 (2.3)
	P_{bg}	4.3 (2.0)	5.7 (2.3)	3.9 (1.3)	5.2 (2.6)
PC3	ε_{hit}	92.1 (2.9)	94.4 (2.1)	95.1 (2.5)	95.3 (2.3)
	P_{bg}	4.7 (2.3)	6.0 (2.2)	4.0 (1.4)	5.4 (2.6)
PC4	ε_{hit}	93.1 (3.2)	94.5 (2.3)	94.4 (3.1)	95.1 (2.5)
	P_{bg}	5.3 (2.9)	6.7 (2.4)	4.3 (1.8)	5.9 (2.7)

Note. The number in brackets are RMS of distribution of the corresponding parameters for separate cells in superlayer. Statistical errors are negligible due to a big number of events in the sample. The Monte-Carlo simulation has been performed with a hit efficiency of 95 %.

Table 4. Hit efficiency for the data (in %) for PC superlayers corrected on bias estimates from Monte-Carlo simulation

Superlayer	Soft cuts		Strong cuts	
	5 mm	10 mm	5 mm	10 mm
PC1	93.7	94.0	95.7	96.3
PC2	94.1	96.0	96.7	97.6
PC3	93.7	96.2	96.2	97.9
PC4	94.6	94.5	96.0	95.0

The results obtained by Monte-Carlo simulation were used to correct the values of the hit efficiencies obtained from the real data. We add the bias estimation from the Monte-Carlo simulation, i. e., the difference between the input value 95 % and the value in Table 3, to the corresponding value in Table 1. The corrected values of hit efficiency for the both soft and strong cuts are presented in Table 4. There is still some discrepancy between the efficiency estimated with the soft and strong cuts even after taking into account the Monte-Carlo corrections. The value of this discrepancy gives some indication of the systematic error of the method.

CONCLUSION

In this paper we have presented a method for the efficiency determination based on the efficiency profile for separate cells, using tracks selected after standard reconstruction. This

method has been applied for a systematic study of hit efficiency of the OTR PC chambers of the HERA-B main tracker [3]. A fitting function with six parameters has been used for the experimental efficiency profile and to determine the cell efficiency and background probability parameter. The average hit efficiency as well as the value of the background probability for the superlayer has been estimated as an average of the distribution of these parameters for cells in the superlayer.

In the present study the systematic error of the method can be guessed as a discrepancy between the hit efficiency values obtained with two sets of the track-selection cuts. The bias caused by the usage of the hit in the cell under study in the track finding has been estimated and does not exceed 1 %.

REFERENCES

1. *Lohse T. et al.* HERA-B, an Experiment to Study CP Violation in the B System Using an Internal Target at the HERA Proton Ring. DESY-PRC 94/02. Hamburg, 1994.
2. *Spiridonov A.* Track Reconstruction in the High Rate Environment of the HERA-B Spectrometer // Proc. of CHEP 2001, Sept. 2001, Beijing, China / Ed. H. S. Chen. Beijing; N. Y., 2001. P. 168.
3. *Abyzov A. et al.* Study of the Hit Efficiency of the OTR PC Chambers. HERA-B Note 02-034. OTR 02-004. Hamburg, 2002.
4. *Lanyov A.* Modular OTR Geometry Description in ARTE. HERA-B Note 97-259. Zeuthen, 1997.
5. *Mankel R.* A Concurrent Hit Evolution Algorithm for Pattern Recognition in the HERA-B Main Tracking System // Nucl. Instr. Meth. A. 1997. V. 395. P. 169;
Mankel R., Spiridonov A. Ranger — a Pattern Recognition Algorithm for the HERA-B Main Tracker System. Part III: Tracking in Trigger Chambers. HERA-B Note 98-206. Zeuthen, 1998.
6. *Albrecht H.* ARTE (Analysis and Reconstruction Tool). HERA-B Note 95-065. Hamburg, 1995; <http://www-hera-b.desy.de/subgroup/software/arte/>

Received on September 10, 2002.